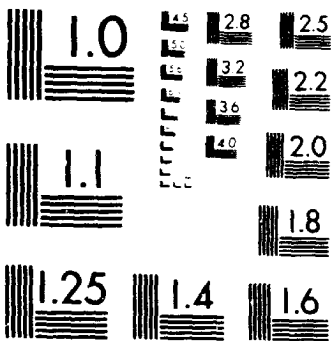


10468 U



MICROCOPY RESOLUTION TEST CHART
NATIONAL BUREAU OF STANDARDS-1963-A





Technical Memorandum 79648

(NASA-10-79648) MAGSAT: VECTOR
MAGNETOMETER ABSOLUTE SENSOR ALIGNMENT
DETERMINATION (NASA) 39 1 HC 403/ME A01

882-18400

OSCE 14B

UNCLAS

63/43 39289

MAGSAT - Vector Magnetometer Absolute Sensor Alignment Determination

M. H. Acuna

SEPTEMBER 1981

National Aeronautics and
Space Administration

Goddard Space Flight Center
Greenbelt, Maryland 20771



MAGSAT VECTOR MAGNETOMETER-ABSOLUTE SENSOR
ALIGNMENT DETERMINATION

M. H. Acuña
NASA/Goddard Space Flight Center
Laboratory for Extraterrestrial Physics
Planetary Magnetospheres Branch
Greenbelt, Maryland 20771

ABSTRACT

This paper discusses a procedure by which the absolute alignment of the magnetic axes of a triaxial magnetometer sensor with respect to an external, fixed, reference coordinate system, can be accurately determined.

The procedure does not require that the magnetic field vector orientation, as generated by a triaxial calibration coil system, be known to better than a few degrees from its true position, and minimizes the number of positions through which a sensor assembly must be rotated to obtain a solution.

Computer simulations have shown that accuracies of better than 0.4 seconds of arc can be achieved under typical test conditions associated with existing magnetic test facilities.

The basic approach is similar in nature to that presented by McPherron and Snare (1978) except that only three sensor positions are required and the system of equations to be solved is considerably simplified. Applications of the method to the case of the MAGSAT Vector Magnetometer are presented and the problems encountered discussed.

INTRODUCTION

The problem of determining the absolute orientation of a magnetic field vector has been solved traditionally by assuming that the field orientation can be accurately established by the geometry of a calibration coil. This method is generally sufficient to determine sensor orientations to within a few minutes of arc from its true direction but if higher accuracies are required not only must we take into account additional parameters in the coil geometry and its construction, but also its time and temperature stability.

A straightforward method of determining the absolute orientation of a magnetic field vector is by rotation of a fluxgate magnetometer sensor (or any other vector sensor) on a surface about an axis approximately parallel to the field direction. The surface orientation can then be adjusted to obtain a constant reading, independent of rotation angle. It can easily be shown that

under these conditions the surface normal, as measured with respect to a reference coordinate system, is parallel to the applied magnetic field vector. It is obvious that for maximum sensitivity, the field must be applied approximately normal to the sensor axis.

A major drawback of this approach is the fact that accurate planar rotations can only be obtained about the local vertical axis due to gravity effects on the support structures. In addition the method is extremely time consuming and requires complex support instrumentation such as non-magnetic, precision, 3-degrees-of-freedom fixtures of performance comparable to first order theodolites.

The procedure presented below obviates the need for multiple rotations and special mounting fixtures and allows the simultaneous determination of the sensor assembly and test coil facility alignment parameters by means of a simple iterative algorithm and measurements obtained for three discrete and fixed sensor positions. Variations with time and temperature of test coil orientations do not affect the determination of the sensor alignment if their characteristic time is long compared with the test time. Thus significant savings in test time are realized since many sources of error which otherwise would have to be accounted for in a rather complex and interacting scheme, are eliminated.

ALIGNMENT DETERMINATION METHOD

The basic assumption in the method is that if the deviations from orthogonality of the sensor assembly and test coils are small (within a few degrees) the measurements obtained from a sensor mounted normal to the field direction will reflect the sum of the deviations of the sensor and test coil system.

A reference coordinate system is first accurately established by a pair of first order theodolites which are rigidly mounted to suitable supports, leveled and referenced to a stable azimuth direction. The coil system orientation is approximately aligned with the reference coordinate system and the magnetic field vectors in the reference and coil coordinate systems are related by

$$\vec{H}_R = [B] \vec{H}_C \quad (1)$$

where $[B] = [I]$ (unit matrix) if the systems are nearly aligned. Thus, in general, $|B_{ij}| \ll 1$ for $i \neq j$.

In analogous fashion we define a matrix $[A]$ which relates the measurements in the sensor coordinate system to the reference coordinate system

$$\vec{M}_S = [A] \vec{M}_R \quad (2)$$

where \vec{M}_S is the measured field vector. Again, if we assume near alignment, $|A_{ij}| \ll 1$ for $i \neq j$ and $|A_{ii}| \approx 1$.

The problem then reduces to determining the elements of $[A]$ from a set of measurements obtained by varying \vec{H}_C and $[A]$ in a known way. This can be accomplished by energizing one axis of the coil system at a time and reorienting the sensor assembly to exchange rows or columns of $[A]$.

In general then we have

$$\vec{M}_S = [A] \vec{M}_R = [A] [B] \vec{H}_C \quad (3)$$

Since the coils are energized one axis at a time and restricting ourselves to unit magnitude vectors, we can write \vec{H}_C as a unit matrix

$$\vec{H}_C \equiv [\vec{H}_C] = \begin{bmatrix} 1 & 0 & 0 \\ 0 & 1 & 0 \\ 0 & 0 & 1 \end{bmatrix} = [I] \quad (4)$$

It then follows that the measurements can be organized in a 3×3 matrix such that

$$[\vec{M}_S] = [A] [B] \quad (5)$$

Under the assumption that the off-diagonal elements of $[A]$ and $[B]$ are small, we can rewrite (5) as

$$[M_S] = [I + \delta A] [I + \delta B] \quad (6)$$

and neglecting second order terms,

$$[M_S] = [I] + [\delta A] + [\delta B] \quad (7)$$

It is worthwhile to express (7) in component form and we shall use the superscript (1) to indicate that these values correspond to the first sensor position (axes nearly parallel to test coils axes)

$$[M_S]^{(1)} = \begin{bmatrix} M_{xx}^{(1)} & M_{xy}^{(1)} & M_{xz}^{(1)} \\ M_{yx}^{(1)} & M_{yy}^{(1)} & M_{yz}^{(1)} \\ M_{zx}^{(1)} & M_{zy}^{(1)} & M_{zz}^{(1)} \end{bmatrix} = \begin{bmatrix} 1 & (a_{xy}+b_{xy}) & (a_{xz}+b_{xz}) \\ (a_{yx}+b_{yx}) & 1 & (a_{yz}+b_{yz}) \\ (a_{zx}+b_{zx}) & (a_{zy}+b_{zy}) & 1 \end{bmatrix} \quad (8)$$

The first subscript of M_{ij} denotes the sensor axis being read while the second denotes the coil system axis (i.e., x, y, z) which is energized. The same convention applies to the elements of the matrices [A] and [B].

If we now rotate the sensor assembly about the z-axis of the reference system, by exactly 90° , the matrix [A] will now take the form

$$[A]^{(2)} = \begin{bmatrix} -a_{xy} & a_{xx} & a_{xz} \\ -a_{yy} & a_{yx} & a_{yz} \\ -a_{zy} & a_{zx} & a_{zz} \end{bmatrix} \quad (9)$$

where we have denoted by $[A]^{(2)}$ the resultant matrix. Note that this rotation can be easily accomplished by means of reference theodolites and optical cubes mounted on the sensor assembly, as described later on in this paper.

If we now energize the coil system axes in the same order as before we have

$$[M_S]^{(2)} = [A]^{(2)} [B] \quad (10)$$

or, in component form

$$[M_S]^{(2)} = \begin{bmatrix} M_{xx}^{(2)} & M_{xy}^{(2)} & M_{xz}^{(2)} \\ M_{yx}^{(2)} & M_{yy}^{(2)} & M_{yz}^{(2)} \\ M_{zx}^{(2)} & M_{zy}^{(2)} & M_{zz}^{(2)} \end{bmatrix} = \begin{bmatrix} (-a_{xy}+b_{yx}) & (a_{xy}+b_{yz}) & 1 \\ -1 & (a_{yz}-b_{xz}) & (a_{yx}-b_{xy}) \\ (-a_{zy}+b_{zx}) & 1 & (a_{zx}+b_{zy}) \end{bmatrix} \quad (11)$$

where the upperscript (2) denotes sensor position number 2. Equations (9) and (11) constitute a system of 12 equations in 12 unknowns but as shown by McPherron and Snare (1978) the characteristic matrix of the system is singular. Thus an additional sensor rotation is required. We choose to rotate the sensor exactly 90° about the X-axis of the reference system. The sensor alignment matrix then becomes

$$[A]^{(3)} = \begin{bmatrix} -a_{xy} & -a_{xz} & a_{xx} \\ -a_{yy} & -a_{yz} & a_{yx} \\ -a_{zy} & -a_{zz} & a_{zx} \end{bmatrix} \quad (12)$$

Energizing the coil system axes in sequence we obtain

$$[\hat{M}_S]^{(3)} = \begin{bmatrix} M_{xx}^{(3)} & M_{xy}^{(3)} & M_{xz}^{(3)} \\ M_{yx}^{(3)} & M_{yy}^{(3)} & M_{yz}^{(3)} \\ M_{zx}^{(3)} & M_{zy}^{(3)} & M_{zz}^{(3)} \end{bmatrix} = \begin{bmatrix} (-a_{xy}+b_{zx}) & (-a_{xz}+b_{zy}) & 1 \\ -1 & (-a_{yz}-b_{xy}) & (a_{yx}-b_{xz}) \\ (-a_{zy}-b_{yz}) & -1 & (a_{zx}-b_{yz}) \end{bmatrix} \quad (13)$$

where the upperscript (3) denotes sensor position number 3. It is clear that equations (8), (11) and (13) allow the twelve coefficients a_{ij} , b_{ij} ($i \neq j$) to be estimated. The diagonal elements a_{ii} and b_{ii} have to satisfy the direction cosine constraints.

$$a_{ii} = [1 - (\sum_{\substack{j=1 \\ i \neq j}}^3 a_{ij}^2)]^{1/2} \quad (14)$$

and

$$b_{ii} = [1 - (\sum_{\substack{j=1 \\ i \neq j}}^3 b_{ij}^2)]^{1/2} \quad (15)$$

and hence can be calculated from the solution of (8), (11), and (13).

Note that it is not necessary to simultaneously solve these equations, since (8) and (11) allow a_{zx} , a_{zy} , b_{zy} , a_{xz} , a_{yz} , b_{xz} and b_{yz} to be determined while the remaining coefficients can be determined using (11) and (13).

It is then convenient to express the solutions as a set of four systems of linear equations, as follows

$$[C_{1j}] = \begin{bmatrix} -1 & 0 & 1 & 1 \\ -1 & 0 & 0 & 1 \\ 0 & -1 & 0 & -1 \\ 0 & -1 & 1 & 0 \end{bmatrix}^{-1} \begin{bmatrix} (3) \\ M_{xx} \\ (2) \\ M_{xx} \\ (3) \\ M_{zx} \\ (2) \\ M_{zx} \end{bmatrix} \quad (16)$$

$$[C_{2j}] = \begin{bmatrix} 1 & 0 & 1 & 0 \\ 1 & 0 & 0 & 1 \\ 0 & -1 & 1 & 0 \\ 0 & 1 & 0 & 1 \end{bmatrix}^{-1} \begin{bmatrix} (1) \\ M_{zx} \\ (2) \\ M_{zy} \\ (2) \\ M_{zx} \\ (1) \\ M_{zy} \end{bmatrix} \quad (17)$$

$$[C_{3j}] = \begin{bmatrix} 1 & 0 & 1 & 0 \\ 0 & 1 & 0 & 1 \\ 1 & 0 & 0 & 1 \\ 0 & 1 & -1 & 0 \end{bmatrix}^{-1} \begin{bmatrix} M_{xz} \\ (1) \\ M_{yz} \\ (2) \\ M_{xz} \\ (2) \\ M_{yz} \end{bmatrix} \quad (18)$$

$$[C_{4j}] = \begin{bmatrix} 1 & 0 & -1 & 0 \\ 1 & 0 & 0 & -1 \\ 0 & -1 & 0 & -1 \\ 0 & 1 & -1 & 0 \end{bmatrix}^{-1} \begin{bmatrix} (3) \\ M_{yz} \\ (2) \\ M_{yy} \\ (3) \\ M_{yy} \\ (3) \\ M_{yz} \end{bmatrix} \quad (19)$$

with $j = 1, \dots, 4$

We then form the estimated matrices

$$[A]_{\text{est}}^{(1)} = \begin{bmatrix} A_{11} & C_{11} & C_{31} \\ C_{41} & A_{22} & C_{32} \\ C_{21} & C_{22} & A_{32} \end{bmatrix} \quad (20)$$

with

$$A_{11} = [1 - (C_{11}^2 + C_{31}^2)]^{1/2}$$

$$A_{22} = [1 - (C_{41}^2 + C_{32}^2)]^{1/2} \quad (21)$$

$$A_{33} = [1 - (C_{21}^2 + C_{22}^2)]^{1/2}$$

and

$$\begin{bmatrix} C_{23} & C_{24} & B_{33} \end{bmatrix}$$

with

$$\begin{aligned} B_{11} &= [1 - (C_{44}^2 + C_{33}^2)] \\ B_{22} &= [1 - (C_{14}^2 + C_{34}^2)] \\ B_{33} &= [1 - (C_{23}^2 + C_{24}^2)] \end{aligned} \quad (23)$$

These matrices $[A]_{\text{est}}$ and $[B]_{\text{est}}$ represent our first attempt to determine the exact solution and hence, at this stage of the calculation we will have

$$[\hat{M}_S]^{(i)} \neq [A]_{\text{est}} [B]_{\text{est}} \quad (i) \quad (24)$$

$$i = 1, 2, 3$$

To improve our estimates we can utilize (24) to implement an iterative scheme which will converge to the desired result $[\hat{M}_S]^{(i)} = [A]_{\text{est}}^{(i)} [B]_{\text{est}}$.

To accomplish this we first form the estimated matrices

$$[A]_{\text{est}} = \begin{bmatrix} -A_{12} & A_{11} & A_{13} \\ -A_{22} & A_{21} & A_{23} \\ -A_{32} & A_{31} & A_{33} \end{bmatrix} \quad (25)$$

and

$$[A]_{\text{est}} = \begin{bmatrix} -A_{12} & -A_{13} & A_{11} \\ -A_{22} & -A_{23} & A_{21} \\ -A_{32} & -A_{33} & A_{31} \end{bmatrix} \quad (26)$$

where the A_{ij} 's are elements of the matrix $[A]_{est}$. We then obtain the products

$$\begin{aligned} [\hat{M}_S]_{est}^{(1)} &= [A]_{est}^{(1)} [B]_{est} \\ [\hat{M}_S]_{est}^{(2)} &= [A]_{est}^{(2)} [B]_{est} \\ [\hat{M}_S]_{est}^{(3)} &= [A]_{est}^{(3)} [B]_{est} \end{aligned} \quad (27)$$

and the differences with the measured values

$$\begin{aligned} \Delta \hat{M}_1 &= [\hat{M}_S]^{(1)} - [\hat{M}_S]_{est}^{(1)} \\ \Delta \hat{M}_2 &= [\hat{M}_S]^{(2)} - [\hat{M}_S]_{est}^{(2)} \\ \Delta \hat{M}_3 &= [\hat{M}_S]^{(3)} - [\hat{M}_S]_{est}^{(3)} \end{aligned} \quad (28)$$

We then solve equations (14) through (17) utilizing the updated values of $[\hat{M}_S]^{(1)}$, $[\hat{M}_S]^{(2)}$ and $[\hat{M}_S]^{(3)}$ defined by

$$\begin{aligned} [\hat{M}_S]^{(1)} &= [\hat{M}_S]_{est}^{(1)} + \Delta \hat{M}_1 \\ [\hat{M}_S]^{(2)} &= [\hat{M}_S]_{est}^{(2)} + \Delta \hat{M}_2 \\ [\hat{M}_S]^{(3)} &= [\hat{M}_S]_{est}^{(3)} + \Delta \hat{M}_3 \end{aligned} \quad (29)$$

kth iteration (k-1)_{th} iteration

until the smallest element of $\Delta \hat{M}_1$, $\Delta \hat{M}_2$ or $\Delta \hat{M}_3$ does not exceed a predetermined small value typically chosen as 10^{-9} . When this condition is satisfied we consider $[A]_{est}$ and $[B]_{est}$ to be the desired solution.

Note that in equation (28) the value of $[\hat{M}_S]^{(1)}$, $[\hat{M}_S]^{(2)}$ and $[\hat{M}_S]^{(3)}$ remain constant during the iteration procedure since they represent the actual measurements.

It is instructive at this point to compare the present method with that given by McPerron and Snare (1973). The basic difference is the method of solution of the approximate equation (7). In their paper they state that a minimum of four different orientations of the sensor are required which lead to a system of 36 equations in 12 unknowns. The solution of this system is implemented using the singular value decomposition method of Lanzcos. In the present method, the solution of equations (15) through (19) is trivial and only three sensor positions are required, considerably simplifying the measurements task.

COMPUTER SIMULATIONS

The procedure presented in the preceding section was programmed on an IBM 5100 computer utilizing the APL language (IBM, 1977). This simulation program is shown in Appendix A. The inputs to the program were two matrices [A] and [B] representing the coil and sensor misalignments. Representative values for [A] and [B] were chosen and the theoretical measurement value computed. These values were in turn used to recover the alignment matrices [A] and [B] with the method presented.

Two examples are shown in Tables I and II. The first represents typical values expected in the case of the MAGSAT Vector Magnetometer and a typical coil system. [A] and [B] are the input matrices and [SV] and [BV] the corresponding estimated matrices. As can be observed the input matrices were recovered exact to the 10th decimal place in only 3 iterations. The second example (Table II) represents an extreme case where angular misalignments as large as 16.7° were allowed for the sensor matrix. Again, the procedure recovered the input matrices with an accuracy of 7×10^{-10} in only 6 iterations.

For these two examples we have assumed that the measurements are error free. Below we discuss several sources of error and their effect upon the overall accuracy of the alignment determination.

ERROR SOURCES AND THEIR IMPACT ON OVERALL ACCURACY

Two fundamental measurement limitations must be taken into account to estimate the overall accuracy of any alignment method and they are: a) resolution and b) noise. We will discuss later additional sources of error which fortunately can be adequately accounted for by the alignment determination method.

The resolution with which we can obtain the measurements establishes a minimum value of signal that can be reliably detected. For the MAGSAT case this was not a limitation because the measurements were obtained with 6 digit resolution. Thus in the absence of noise, we theoretically resolved 0.1 μV of signal which corresponds to 1 part in 4000 (the calibration constant for the instrument was 4 mv/nT or 2.5×10^{-4} nT in a field of 50,000 nT, which corresponds to an angular error of 1×10^{-3} seconds of arc. However, noise, in both the coil system and magnetometer, constitutes a more fundamental limitation. Typical values of noise were 0.1 nT RMS for the coil system "zero" field and 0.01 nT RMS for the magnetometer. Thus, it became extremely important to minimize the calibration facility noise.

For purposes of discussion let's assume that the "noise" (including all contributions) can be reduced to 0.05 nT by suitable procedures with a worst case value of 0.1 nT. If the test field is 50,000 nT, this implies that angular deviations smaller than 0.2 seconds of arc, with a worst case value of 0.4 seconds of arc, cannot be reliably detected.

These effects were simulated in the computer program where artificial random "noise" in multiples of 0.4 arc second peak amplitude was added to the theoretical measurements. The results of these simulations are presented in Tables III and IV for the same cases previously presented in Tables I and II. The number of iterations in this case was fixed at six since obviously the 10^{-9} bound for $\Delta \vec{M}_i$ could not be achieved. As expected, the alignment matrices obtained show deviations of the same order of magnitude as the random noise amplitude.

An additional source of error is the accuracy with which the test field can be established. Fortunately a proton precession magnetometer used to determine the absolute value of the field to better than 1 nT which, for the small misalignment angles involved, does not affect the values obtained to any significant extent. However, to illustrate its contribution, let us assume that the sensor and coil system are misaligned by 0.3° and the field is in error by 2 nT. For small angles

$$\Delta\alpha = \frac{\Delta H_c}{H_c} \alpha \quad (30)$$

where α = misalignment angle

$\Delta\alpha$ = deviation of α from true value

H_c = applied field

ΔH_c = deviation of applied field from true value.

The effective angular error introduced is then 0.04 arc seconds for a 50,000 nT test field. As indicated by (30) this error is proportional to the misalignment angle and hence they should be made initially as small as possible. This also implies that the axis of the reference coordinate system should be aligned with the coil system axis as accurately as possible.

An additional source of error which must be minimized is that due to field gradients associated with the coil system. Since the sensor assembly generally cannot rotate about the sensor axes, each rotation results in a slight translation for at least two of the three sensors constituting the triad. This translation is unimportant unless the field gradients are relatively large in which case the sensors are exposed to different fields depending on their position within the coil system. It is clear from the preceding discussion that the field gradient should be less than 0.1 nT across the largest dimension of the sensor assembly to maintain an overall accuracy comparable to that determined by the noise characteristics of the coil system.

Finally, we must consider the effects introduced by the presence of magnetic materials in the immediate vicinity of the coil system which, by induction effects, alter the direction of the "free space" field produced by the coil system. Examples of this problem were the theodolites themselves which incorporate in their construction soft magnetic materials with high effective permeability. Normally, these instruments are mounted remote from the center of the coil system but unfortunately close enough to introduce deviations in the orientation of the generated field of the order of a few arc seconds.

The magnitude of the induction field can easily be determined with a proton precession magnetometer. Since the alignment determination method does not require precise knowledge of the coil system alignment, the theodolites can be considered as integral parts of the system since their geometry and orientation remain fixed during all the magnetic tests. This obviously can be accomplished with great accuracy since first order instruments are generally used for calibration.

APPLICATION TO THE MAGSAT VECTOR MAGNETOMETER

The sensor assembly for the MAGSAT Vector Magnetometer is shown in Figure 1. Three ring core fluxgate sensors are mounted orthogonally on a glass-ceramic base. Two optical cubes were bonded to the sensor assembly as illustrated in the figure and the relative alignment of the cube faces measured with a set of first order theodolites. A description of the magnetometer overall design and electronics has been given by Acuna et al., 1978 and Acuna, 1980 so it will not be repeated here.

The calibration and alignment tests were conducted at the Goddard Space Flight Center 6 meter Magnetic Test Facility. Two concrete piers separated by approximately 400 meters established an optical azimuth reference, as shown in Figure 2. This base line was used to verify the absolute azimuthal orientation of two first order theodolites mounted inside the coil building which established the primary, orthogonal, reference coordinate system. The system was verified periodically by means of auxiliary mirrors and found to yield

repeatable results with a typical uncertainty of less than 2 arc-seconds. The facility was equipped with a state-of-the-art servo control system to monitor and correct earth's field variations in the range of 0 to 25 Hz. The typical noise level of the system was 0.1 nT RMS. All calibration activities took place during selected "quiet" evenings to minimize errors due to refraction effects by hot air currents and other significant disturbances such as nearby electric railroad traffic and wind induced distortions of the coil building. The computer programs described in Appendix 'A' were modified and expanded as shown in Appendix 'B' for these tests.

During engineering model tests the effects of cross-field non-linearities in ring-core fluxgate sensors were evaluated and found to be significant for fields greater than 15,000 nT. This problem is shown in Figure 3. Ring core fluxgate magnetometers with large effective (L/d) ratios exhibit deviations from linearity of the order of 1 part in 10^5 for fields applied parallel to the sensitive axis. This figure degrades significantly when a large field is simultaneously applied in a direction transverse to the sensing axis, as shown in Figure 3. This is due to the appearance of large amplitude second harmonic signals at the sensor terminals which are in phase quadrature with the signal produced by the on-axis field. These large signals affect the linear operation of the electronics and lead to the observed instrument response. Note that the response function depends upon the applied on-axis and cross-axis fields.

The strategy followed for MAGSAT was to mathematically model out these non-linearities rather than correct them in the instrumentation. To determine the dependence of the alignment angles with the amplitude of the test field caused by the non-linear response, the method described in the previous section was used with test fields of 55,000 nT, 35,000 nT and 15,000 nT. As expected, the results obtained for the sensor alignment matrix did vary with the amplitude of the test field, but not those for the test coil system alignment matrix. This, of course, is what would be anticipated since the coil system alignment matrix is test-field amplitude independent.

One important fact derived from the measurements was that only those matrix elements associated with directions in the plane of a given sensor ring

core were field amplitude dependent. This is not surprising since in the direction perpendicular to the plane of the core there exists a large demagnetizing factor due to the narrow ring-core-sensor geometry and resulting small (l/d) ratio (Bozorth, 1951; Acuna, 1969).

Thus we can write

$$[A] = \begin{bmatrix} A_{xx} & A_{xy}(B_x, B_y) & A_{xz} \\ A_{yx}(B_x, B_y) & A_{yy} & A_{yz} \\ A_{zx} & A_{zy}(B_z, B_y) & A_{zz} \end{bmatrix} \quad (31)$$

The functions $A_{ij}(B_i, B_j)$ constitute second order corrections to the basic measurements and hence are not strong functions of B . Thus for all practical purposes choosing $B_i = B_{\text{measured } i}$ (raw) in (31) above does not introduce any significant errors in the determination of the A_{ij} terms. Typical results obtained for A_{ij} 's as a function of the test field amplitude are given in Table 5.

The measurements were least squares fitted to functions of the form

$$A_{ij}(B_i, B_j) = \frac{A_{ij}}{B_j} \sin \frac{\alpha_{ij} B_j}{A_{ij}} \quad (32)$$

for A_{12} , A_{21} and A_{31} with excellent results. Now (32) only models the response to cross-axis fields without regard for the magnitude of the on axis field. Hence (32) must be expanded to include this dependence

$$A_{ij}(B_i, B_j) = \frac{A_{ij}(B_i)}{B_j} \sin \frac{\alpha_{ij} B_j}{A_{ij}(B_i)} \quad (33)$$

The functional form of $A_{ij}(B_i)$ was determined experimentally by full 4 π steradian mapping of the instrument response function. The following functional relation was found to fit the measurements with the required accuracy

$$A_{ij}(B_i) = C_0 + C_1 A_i \frac{B_j}{|B_j|} + C_2 \exp(C_3 B_i \frac{B_j}{|B_j|}) \quad (34)$$

The final values derived for the MAGSAT flight sensor coefficients are given in Table 6. The final absolute alignment accuracy achieved through the measurement and modeling activity was estimated at ± 3 arc seconds.

SUMMARY

A relatively simple procedure to accurately determine the absolute alignment of vector magnetometer sensors has been presented. The method minimizes the number of sensor orientations necessary to obtain a solution and requires simple mathematical operations. Computer simulations have demonstrated the rapid convergence of the solutions to exceedingly small values of error, even for initial deviations from orthogonality as large as 16 degrees. Several error sources limiting the obtainable accuracy in practical applications were presented and it was shown that angular determination accuracies of the order of 0.4 arc seconds are technically achievable. Finally, the application of the method to the MAGSAT Vector Magnetometer alignment was presented including second order effects associated with large (t/d) ring core fluxgate sensors.

REFERENCES

- Acuna, M. H., "A Miniature Two-axis Fluxgate Magnetometer", IEEE Trans. on Geoscience Electronics, GE-7, Number 4, October 1969.
- Acuna, M. H., C. S. Searce, J. B. Seek and J. Scheifele, "The MAGSAT Vector Magnetometer - A Precision Fluxgate Magnetometer for the Measurement of the Geomagnetic Field", NASA Technical Memorandum 79656 (1978).
- Acuna, M. H., "The MAGSAT Precision Vector Magnetometer", APL Technical Digest, Vol. 1, Number 3, 1980.
- Bozorth, R. M., "Ferromagnetism", D. Van Nostrand Co. Pub., Princeton, N.J., 1951.
- IBM, "IBM 5100 - APL Reference Manual", Pub. No. SA21-9213-3, June 1977.
- R. L. McPherron and R. C. Snare, "A Procedure for Accurate Calibration of the Orientation of the three Sensors in a Vector Magnetometer", IEEE Trans. Geoscience Electronics, Vol. GEO-16 2, 134-137, April 1978.

FIGURE CAPTIONS

Figure 1 - Schematic representation of the MAGSAT Vector magnetometer triaxial sensor assembly. Three ring-core fluxgate sensors are mounted orthogonal to each other. Two optical cubes bonded to the assembly define the reference coordinate system.

Figure 2 - The MAGSAT optical reference system as implemented at the NASA-GSFC 6-meter Magnetic Test Facility. The 400-meter baseline stability was checked periodically against stellar references.

Figure 3 - Response of large (l/d)-ratio ring-core fluxgate sensors to cross and on-axis fields simultaneously, applied in the plane of the core. The deviations from linearity are produced by large quadrature signals generated by the sensor under these conditions (large external fields). For external field < 5000 nT the effect is negligible.

TABLE 1

MAGSATSIM 0
ENTER SIMULATED SENSOR ALIGNMENT MATRIX
Q:

A
ENTER SIMULATED COIL ALIGNMENT MATRIX
Q:

B
AZY, BZX, AYZ, BXZ : 0.0089995 -0.00036744 -0.0070028 -0.00012528
AZY, BZX, AYZ, BXZ : 0.0089984 -0.00036861 -0.007004 -0.00012403
AZY, BZX, AYZ, BXZ : 0.0089984 -0.00036861 -0.007004 -0.00012403

A
0.99999 0.002 -0.003
0.0056 0.99996 -0.007
0.0001 0.009 0.99996

B
1.0000E0 2.0000E-4 -1.2000E-4
5.3000E-5 1.0000E0 4.5000E-4
-3.6700E-4 3.8900E-4 1.0000E0

SV
9.9999E-1 2.0000E-3 -3.0000E-3
5.6000E-3 9.9996E-1 -7.0000E-3
1.0000E-4 9.0000E-3 9.9996E-1

BV
1.0000E0 2.0000E-4 -1.2000E-4
5.3000E-5 1.0000E0 4.5000E-4
-3.6700E-4 3.8900E-4 1.0000E0

} ≡ A_{est}

} ≡ B_{est}

TABLE II

MAGSATSIM 0
ENTER SIMULATED SENSOR ALIGNMENT MATRIX
D:

A
ENTER SIMULATED COIL ALIGNMENT MATRIX
D:

B
AZY, BZX, AYZ, BXZ : 0.11 1.1154E-5 0.30003 4.7675E-6
AZY, BZX, AYZ, BXZ : 0.10997 3.9936E-5 0.30005 8.0389E-6
AZY, BZX, AYZ, BXZ : 0.10997 4.0079E-5 0.30005 8.6579E-6
AZY, BZX, AYZ, BXZ : 0.10997 4.0274E-5 0.30005 8.7035E-6
AZY, BZX, AYZ, BXZ : 0.10997 4.0278E-5 0.30005 8.7113E-6
AZY, BZX, AYZ, BXZ : 0.10997 4.028E-5 0.30005 8.712E-6

A
0.97468 0.1 -0.2
0.05 0.95263 -0.3
0.005 -0.11 0.99392

B
1.0000E0 5.0000E-4 4.0000E-5
3.0000E-6 1.0000E0 2.0000E-4
1.0000E-5 4.5000E-5 1.0000E0

SV
0.97468 0.1 -0.2
0.05 0.95263 -0.3
0.005 -0.11 0.99392

BV
1.0000E0 5.0000E-4 4.0000E-5
2.9993E-6 1.0000E0 2.0000E-4
1.0000E-5 4.5000E-5 1.0000E0

TABLE III

MAGSATSIM 1

ENTER SIMULATED SENSOR ALIGNMENT MATRIX

D:

A

ENTER SIMULATED COIL ALIGNMENT MATRIX

D:

B

AZY, BZX, AYZ, BXZ : 0.0089995 -0.00036744 -0.0070028 -0.00012528
 AZY, BZX, AYZ, BXZ : 0.0089982 -0.00036875 -0.007004 -0.00012416
 AZY, BZX, AYZ, BXZ : 0.008998 -0.00036899 -0.0070039 -0.00012412
 AZY, BZX, AYZ, BXZ : 0.0089977 -0.00036924 -0.0070039 -0.00012407
 AZY, BZX, AYZ, BXZ : 0.0089975 -0.00036949 -0.0070038 -0.00012403
 AZY, BZX, AYZ, BXZ : 0.0089972 -0.00036974 -0.0070038 -0.00012398

A

0.99999	0.002	-0.003
0.0056	0.99996	-0.007
0.0001	0.009	0.99996

B

1.0000E0	2.0000E-4	-1.2000E-4
5.3000E-5	1.0000E0	4.5000E-4
-3.6700E-4	3.8900E-4	1.0000E0

SV

0.99999	0.0019997	-0.0029998
0.0055999	0.99996	-0.007
0.0001	0.0090001	0.99996

BV

1.0000E0	1.9978E-4	-1.2017E-4
5.2955E-5	1.0000E0	4.5002E-4
-3.6688E-4	3.8909E-4	1.0000E0

TABLE IV

MAGSATSIM 1
ENTER SIMULATED SENSOR ALIGNMENT MATRIX
D:

A
ENTER SIMULATED COIL ALIGNMENT MATRIX
D:

B
AZY,BZX,AYZ,BXZ : -0.11 1.1154E-5 -0.30003 -4.7675E-6
AZY,BZX,AYZ,BXZ : -0.10997 3.9991E-5 -0.30005 -8.2689E-6
AZY,BZX,AYZ,BXZ : -0.10997 4.0117E-5 -0.30005 -9.0327E-6
AZY,BZX,AYZ,BXZ : -0.10997 4.0295E-5 -0.30005 -9.2234E-6
AZY,BZX,AYZ,BXZ : -0.10997 4.0284E-5 -0.30005 -9.376E-6
AZY,BZX,AYZ,BXZ : -0.10997 4.027E-5 -0.30005 -9.5215E-6

A
0.97468 0.1 -0.2
0.05 0.95263 -0.3
0.005 -0.11 0.99392

B
1.0000E0 5.0000E-4 4.0000E-5
3.0000E-6 1.0000E0 2.0000E-4
1.0000E-5 4.5000E-5 1.0000E0

SV
0.97468 0.1 -0.2
0.05 0.95263 -0.3
0.005 -0.11 0.99392

BV
1.0000E0 4.9978E-4 3.9951E-5
3.1344E-6 1.0000E0 2.0003E-4
1.0051E-5 4.5191E-5 1.0000E0

Test Field Amplitude [nT]

Coefficient	15,000	35,000	55,000
$A_{xy} (B_x=0)$	$- 1.0604 \times 10^{-3}$	$- 9.26198 \times 10^{-4}$	$- 7.10277 \times 10^{-4}$
$A_{xz} (B_x=0)$	7.92×10^{-4}	7.92×10^{-4}	7.92×10^{-4}
$A_{yx} (B_x=0)$	$- 2.868 \times 10^{-3}$	$- 2.61318 \times 10^{-3}$	$- 2.18877 \times 10^{-3}$
$A_{yz} (B_y=0)$	2.208×10^{-3}	2.208×10^{-3}	2.208×10^{-3}
$A_{zx} (B_z=0)$	2.3325×10^{-3}	2.3325×10^{-3}	2.3325×10^{-3}
$A_{zy} (B_z=0)$	$- 2.84214 \times 10^{-3}$	$- 2.65283 \times 10^{-3}$	$- 2.33114 \times 10^{-3}$

		Axis		
	Coefficient	X	Y	Z
C_0	- 37.72	- 119.93	- 136.4	
C_1	1.9808×10^{-4}	4.5333×10^{-4}	4.2×10^{-4}	
C_2	- 1.3679	- 5.65134	- 6.92989	
C_3	- 6.613×10^{-5}	- 5.1848×10^{-5}	- 3.8402×10^{-5}	


```

E341 PF3C3;J+P3C0/2(C1=(P3C;11)*-1/2-3);J
E351 PF3C;11+PF3C;11*(C1=PF3C3;11)-1=PF3C3;11
E361 PF3C;21+PF3C;21*(C1=PF3C1;21)-1=PF3C1;21
E371 PF3C;31+PF3C;31*(C1=PF3C2;31)-1=PF3C2;31
E381 *SIGN NORMALIZED MATRIX FOR POS.#3*)@PF3
E391 B1*AP*QPF1
E401 B2*AP90*QPF2
E411 B3*AP90P*QPF3
E421 I MAGSATSIM 0

```



```

C34] BV+ 3 3 p1,,A5[C4],,A3[C3],,A1[C4],,1,,A3[C4],,A2[C3],,A2[C4],,1
C35] SV[C1,1]+(1-(SV[C1,2])*2)+SV[C1,3]**2)*0.5
C36] SV[C2,2]+(1-(SV[C2,1]**2)+SV[C2,3]**2)*0.5
C37] SV[C3,3]+(1-(SV[C3,1]**2)+SV[C3,2]**2)*0.5
C38] BV[C1,1]+(1-(BV[C1,2]**2)+BV[C1,3]**2)*0.5
C39] BV[C2,2]+(1-(BV[C2,1]**2)+BV[C2,3]**2)*0.5
C40] BV[C3,3]+(1-(BV[C3,1]**2)+BV[C3,2]**2)*0.5
C41] .AZY,BZX,AYZ,BXZ .,JA1[C 3],A5[C 3]
C42] AP+AP+(L1+B1*SV+.*BV)
C43] A90C,1]+-(A90+0(20SV))[,1]
C44] AP90+AP90+(L2<R2-A90+.*BV)
C45] A90PC, 1 2]+-(A90P+10SV)[, 1 2]
C46] AP90P+AP90P+(L3+B3-A90P+.*BV)
C47] .SV,;SV;[NAV[157]; .BV,;BV
C48] I+I+1
C49] +(I=7)/0
C50] +((IML1+AM+,(L1),(L2),(L3))=1E-7)/C01
V

```

```

VMAGC[1]V
V Z←MAG K
[1] Z←K÷ 7 3 ρB
[2] Z←(1↑φZC;1]);1]←ZC(1↑φZC,2]);2]←ZC(1↑φZC;3]);3]←A
[3] Z←(1↑φZC;1]);1]←ZC(1↑φZC,2]);2]←ZC(1↑φZC;3]);3]←--A
[4] Z←(ρ 3 3 ρ--/ 9 2 ρ, ρ 6 3 ρ3↑,Z)÷2
[5] Z←Z÷ 3 3 ρ,A
V

```

```

VERROR[1]V
V A ERROR K;SV2;SV3,T1,T2,T3
[1] B← 3 3 ρ(AxR[1]);0,0,0,(AxR[2]);0,0,0,AxR[3]
[2] 'POSITION #1 RECONST. MEAS'
[3] Π←T1←φ(SV+,xBV)+,xB
[4] SV2C;1]←-(SV2+φ(2φSV))L;1]
[5] 'POSITION #2 RECONST. MEAS'
[6] Π←T2←φ(SV2+,xKV)+,xB
[7] SV3C; 1 2]←-(SV3+1φSV)C; 1 2]
[8] 'POSITION #2 RECONST. MEAS'
[9] Π←T3←φ(SV3+,xKV)+,xB
V

```

APPENDIX B

```

VMEAS[[]]
V A MEAS B;P1;P2;P3
[1] THIS PROGRAM ASSUMES THAT BOTH FIELD POL. ARE APPLIED FOR EACH SENSOR POSITION
[2] A A IS THE TEST FIELD AMPLITUDE AND B ARE THE CALIBRATION FACTORS [VOLTS/GAMMA] X,Y,Z
[3] C03: 'ENTER MEASURED VALUES FOR POSITION #1 (X→D-U),0,U-U,W-E,N-S,X,Y,Z, ORDER'
[4] P1←P1- 7 3 ρ(P1← 7 3 ρP1←[])[1;]
[5] 'DIFFERENCE MATRIX FOR POS.#1';P1
[6] 'ARE VALUES OK? ENTER YES OR NOP'
[7] →((+/0='NOP')=3)/C03
[8] 'NORMALIZED MATRIX FOR POSITION #1';(P1←@MAG P1)
[9] C04: 'ENTER MEASURED VALUES FOR POSITION #2 (X→D-U,Y→N-S)'
[10] P2←P2- 7 3 ρ(P2← 7 3 ρP2←[])[1;]
[11] 'DIFFERENCE MATRIX FOR POSITION #2';P2
[12] 'ARE VALUES OK? ENTER YES OR NOP'
[13] →((+/0='NOP')=3)/C04
[14] 'NORMALIZED MATRIX FOR POS.#2';(P2←@MAG P2)
[15] C05: 'ENTER MEASURED VALUES FOR POS.#3 (X→N-S,Y→U-D)'
[16] P3←P3- 7 3 ρ(P3← 7 3 ρP3←[])[1;]
[17] 'DIFFERENCE MATRIX FOR POS.#3';P3
[18] 'ARE VALUES OK? ENTER YES OR NOP'
[19] →((+/0='NOP')=3)/C05
[20] 'NORMALIZED MATRIX FOR POS.#3';(P3←@MAG P3)
[21] B1←AP←P1
[22] B2←AP90←P2
[23] B3←AP90P←P3
[24] 1 MAGSATSIM 0
[25] 'SENSOR ALIGNMENT MATRIX';SV
[26] 'COIL ALIGNMENT MATRIX';BV

```

V

```

VMAGSATSIM[]V
V A MAGSATSIM K;I;A90;A90P;M1;M2;M3;M5;VA1;VA2;VA3;VA5;A1;A2;A3;A5;M;L1;L2;L3;K1;K2;K3
[1] A IS A CONTROL.1 FOR USE WITH MEAS, 0 FOR STAND ALONE
[2] K1+ 3 3 ρ 0 1 1 1 0 1 1 1 0
[3] K2+ 3 3 ρ 0 1 1 1 1 0 1 0 1
[4] K3+ 3 3 ρ 1 1 0 0 1 1 1 0 1
[5] AK IS RANDOM NOISE IN MULTIPLES OF 0.4''
[6] →(A=1)/CO2
[7] 'ENTER SIMULATED SENSOR ALIGNMENT MATRIX'
[8] A+0
[9] AC[1;1]+(1-(AC[1;2]*2)+AC[1;3]*2)*0.5
[10] AC[2;2]+(1-(AC[2;1]*2)+AC[2;3]*2)*0.5
[11] AC[3;3]+(1-(AC[3;1]*2)+AC[3;2]*2)*0.5
[12] 'ENTER SIMULATED COIL ALIGNMENT MATRIX'
[13] B+0
[14] BC[1;1]+(1-(BC[1;2]*2)+BC[1;3]*2)*0.5
[15] BC[2;2]+(1-(BC[2;1]*2)+BC[2;3]*2)*0.5
[16] BC[3;3]+(1-(BC[3;1]*2)+BC[3;2]*2)*0.5
[17] B1+AP+A+.xB
[18] A90C;3]+-(A90+φ(1φA))C;3]
[19] B2+AP90+A90+.xB
[20] A90PC; 1 3]+-(A90P+1φA)C; 1 3]
[21] B3+AP90P+A90P+.xB
[22] B1+ 3 3 ρ(,B1)+Kx1E-8x9?25
[23] B2+ 3 3 ρ(,B2)+Kx1E-8x9?25
[24] B3+ 3 3 ρ(,B3)+Kx1E-8x9?25
[25] CO2:M1+BM1+ 4 4 ρ 1 0 1 0 0 1 0 1 0 1 1 0 -1 0 0 1
[26] M2+BM2+ 4 4 ρ 1 0 1 0 0 1 0 1 1 0 0 -1 0 1 1 0
[27] M3+BM3+ 4 4 ρ 0 -1 1 0 0 -1 0 1 -1 0 1 0 1 0 0 1
[28] M5+BM5+ 4 4 ρ 0 1 0 -1 1 0 1 0 0 1 -1 0 1 0 0 -1
[29] I+1
[30] CO1:VA1+APC[1;2],APC[1;3],AP90C[1;2],AP90C[1;3]
[31] VA2+APC[2;1],APC[3;1],AP90C[2;1],AP90C[3;1]
[32] VA3+AP90C[3;3],AP90PC[3;1],AP90PC[3;3],AP90C[3;1]

```

```

[33] VA5+AP90[E2,2],AP90[E1,2],AP90PE[2,2],AP90PE[1,2]
[34] A1+M1+.xVA1
[35] A2+M2+.xVA2
[36] A3+M3+.xVA3
[37] A5+M5+.xVA5
[38] SV+ 3 3 p1,,A1[E1],((A1[E2]+A5[E1])÷2),,A2[E1],,1,,A5[E2],((A2[E2]+A3[E1])÷2),,A3[E2],,1
[39] BV+ 3 3 p1,,((A1[E3]+A5[E3])÷2),,A1[E4],,((A2[E3]+A3[E4])÷2),,1,,A3[E3],,A2[E4],,A5[E4],,1
[40] SVE[1;1]+(1-(SVE[1;2]*2)+SVE[1;3]*2)*0.5
[41] SVE[2;2]+(1-(SVE[2;1]*2)+SVE[2;3]*2)*0.5
[42] SVE[3;3]+(1-(SVE[3;1]*2)+SVE[3;2]*2)*0.5
[43] BVE[1;1]+(1-(BVE[1;2]*2)+BVE[1;3]*2)*0.5
[44] BVE[2;2]+(1-(BVE[2;1]*2)+BVE[2;3]*2)*0.5
[45] BVE[3;3]+(1-(BVE[3;1]*2)+BVE[3;2]*2)*0.5
[46] 'A13,B12,A31,B21',,A5[E1 3],A3[E1 4]
[47] AP←AP+(L1+K1×B1-SV+,xBV)
[48] []←(30L1)×360×360÷02
[49] A90[E;3]←-(A90+Φ(1ΦSV))E[,3]
[50] AP90←AP90+(L2+K2×B2-A90+,xBV)
[51] []←(30L2)×360×360÷02
[52] A90PE[;1 3]←-(A90P+1ΦSV)E[;1 3]
[53] AP90P←AP90P+(L3+K3×B3-A90P+,xBV)
[54] []←(30L3)×360×360÷02
[55] 'SV',SV;[]AV[157];'BV',BV
[56] I←I+1
[57] →(I=7)/0
[58] →(([]←(3600×360÷02)×30IM[E1+ΦIM+,(L1),(L2),,L3])≥1)/CO1

```

▽

```

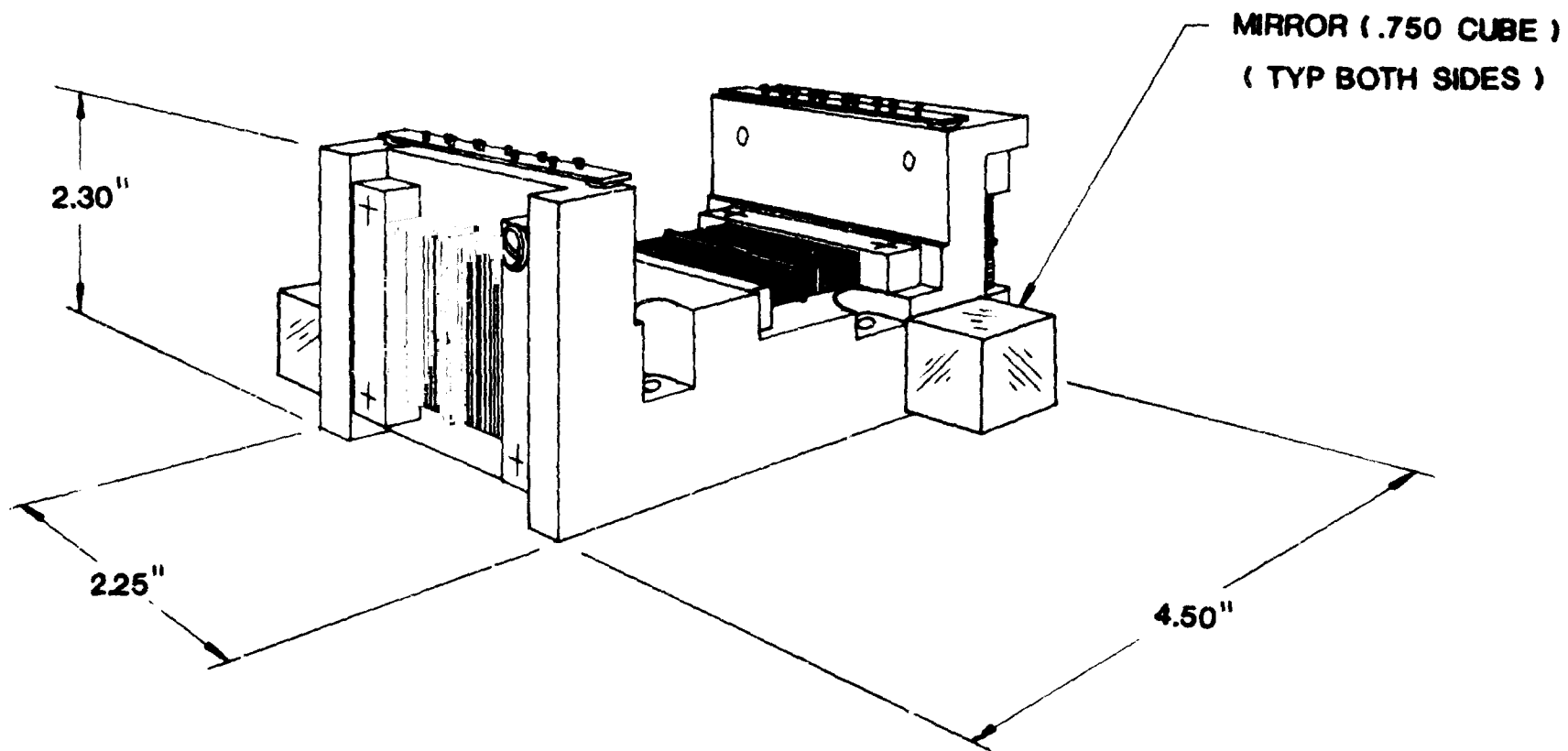
VMAGC(I)V
V Z+MAG K
[1] Z+K- 7 3 pB
[2] ZC(1+ψZC,1);1]+ZC(1+ψZC;2);2]+ZC(1+ψZC;3);3]+A
[3] ZC(1+φZC,1);1]+ZC(1+φZC;2);2]+ZC(1+φZC;3);3]+-A
[4] Z+(Q 3 3 p- / 9 2 p, Q 6 3 p3+,Z)+2
[5] Z+Z- 3 3 p-A

```

```

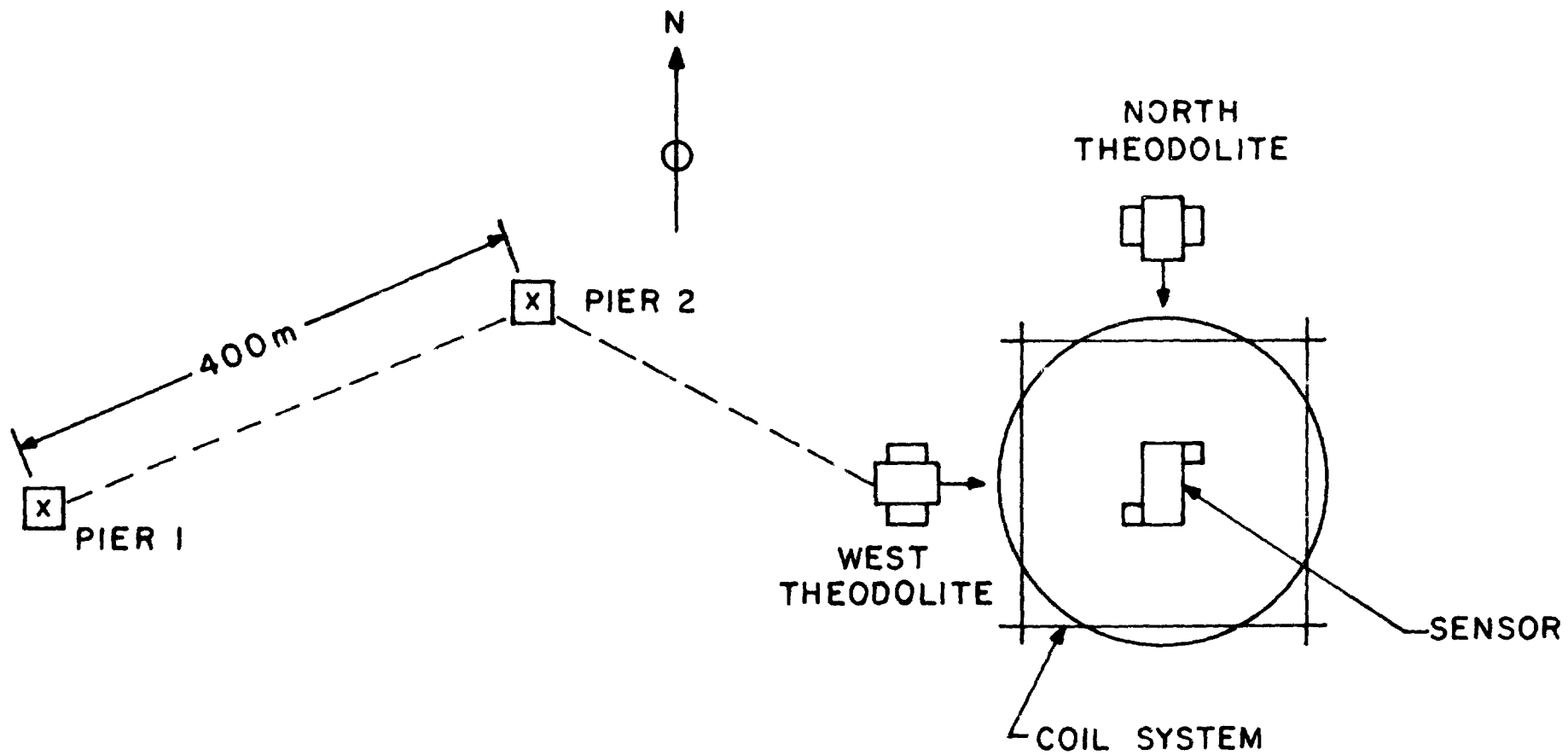
VERROR(I)V
V A FPROR B;SV2,SV3;T1,T2,T3
[1] A IS THE TEST FIELD AMPLITUDE AND B ARE THE CALIBRATION FACTORS
[2] B+ 3 3 p(A×BC1),0,0,0,(A×BC2),0,0,0,A×BC3]
[3] 'POSITION #1 RECONST. MEAS'
[4] []+T1+QB+.x(SV+.xBV)
[5] SV2C,3]+-(SV2+φ(1φSV))C,3]
[6] 'POSITION #2 RECONST. MEAS'
[7] []+T2+QB+.x(SV2+.xBV)
[8] SV3C,1 3]+-(SV3+1φSV)C,1 3]
[9] 'POSITION #3 RECONST. MEAS'
[10] []+T3+QB+.x(SV3+.xBV)

```



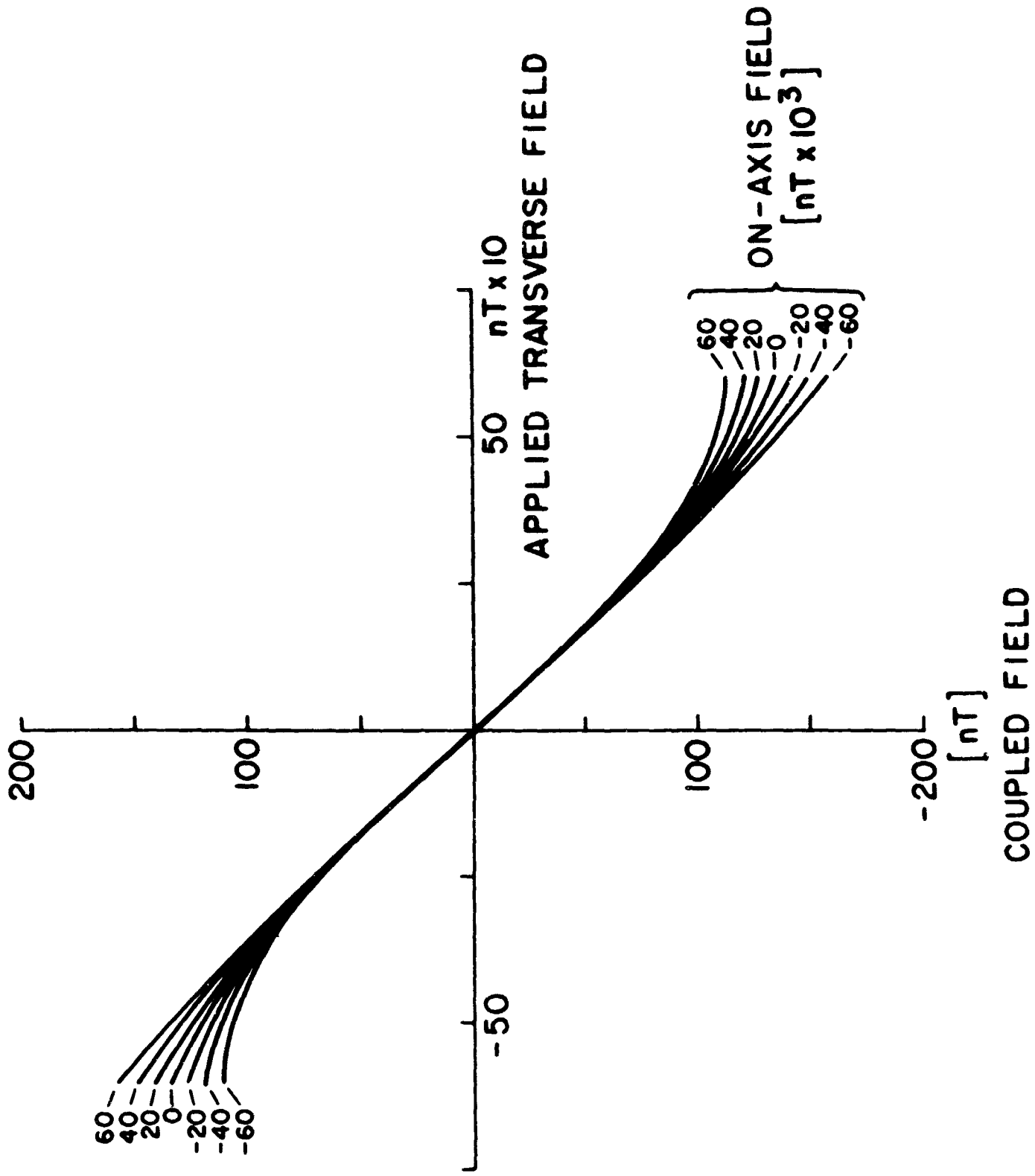
VECTOR MAGNETOMETER SENSOR
MAGSAT

Fig. 1



MAGSAT OPTICAL REFERENCE SYSTEM

fig. 2



END

DATE

FILMED

DEC 23 1981